Kinetic Studies of the Cl + HI Reaction Using Three Techniques

Jessie Yuan,[†] Ashutosh Misra,[‡] A. Goumri, Diane D. Shao, and Paul Marshall*

Department of Chemistry, University of North Texas, P.O. Box 305070, Denton, Texas 76203-5070

Received: June 15, 2004

The reaction Cl + HI → HCl + I was investigated using the laser-photolysis/resonance fluorescence method to monitor (i) the disappearance of atomic Cl and (ii) the growth of atomic I. The results were similar, and together yield the rate constant $k = (3.4 \pm 1.4) \times 10^{-11} \exp (+2.8 \pm 1.1 \text{ kJ mol}^{-1}/RT) \text{ cm}^3 \text{ molecule}^{-1} \text{ s}^{-1}$ (1σ errors) over 297−390 K. The 95% confidence limits for k are ±19%. Another approach, discharge/fast-flow (iii), with monitoring of the consumption of Cl in the presence of excess HI, yields $k = 1.2 \times 10^{-10} \text{ cm}^3$ molecule^{-1} s^{-1} at 298 K, with 95% confidence limits of ±17%. The results are in accord with each other and with most literature data. This indicates that monitoring of the formation of the atomic halogen product in this example of a radical abstraction of H from a hydrogen halide is reliable.

1. Introduction

The fast reaction

$$Cl + HI \rightarrow HCl + I \tag{1}$$

is a well-known infrared chemiluminescent (IRCL) process that has been important in the development of reaction dynamics and investigations of energy disposal.[1,2] We have investigated the thermal rate constant k_1 via three techniques. The temperature dependence of k_1 was evaluated by laser-photolysis/ resonance fluorescence, with monitoring either of (i) the disappearance of Cl, or (ii) the appearance of a product, atomic I. (iii) Consumption of Cl atoms in the presence of excess HI at room temperature was also studied in a discharge flow system. The rate constants obtained here are compared with previous data derived via IRCL[3−6] and relative rate measurements.[7] The main motivation for the present work is to test the reliability of kinetic monitoring of the atomic halogen product X in reactions of the general type

$$R + HX \rightarrow RH + X \tag{2}$$

where R is a radical and where X is readily detectable by resonance fluorescence. Such reactions have been used in the cases of R = alkyl and silyl radicals to obtain kinetic information which, together with data for the reverse reaction, establishes C−H and Si−H bond dissociation enthalpies.[8−10] There have been criticisms of this kind of experiment.[11] These center on the possible influence of excess energy in R when produced photolytically by photons with energies well above the threshold for dissociation of a precursor, the possibility of photochemistry arising from the monitoring radiation, and the need to correct for diffusion effects. Some work involved major (up to 80%) consumption of R by an unknown process that does not produce X, which is speculated to arise from oxygen contamination.[9] This, in turn, raises the possibility of O and O_2 photochemistry.[11] Here, we can monitor both reactant (R = Cl) and product (X =

I) radicals, and check whether the same kinetics are obtained by monitoring I or Cl during reaction 1. As a further check, Cl was monitored both in time-resolved and fast-flow systems.

2. Methodology

2.1 Flash-photolysis Experiments. General operation of our pulsed photolysis reactor has been described elsewhere.[12,13] In this study, Cl_2 was photolyzed to produce Cl radicals by excimer laser (Questek 2010) radiation at 308 nm, and the pulse energy E was measured with a Molectron J25 pyroelectric joulemeter. This chlorine photolysis wavelength takes advantage of the modest UV absorbance of HI at 308 nm,[14] and no atomic iodine was detected when HI alone was subjected to the photolysis beam. The Cl atoms reacted with excess HI to form HCl and I. During the course of the reaction either the decay of [Cl] or the growth of [I] was monitored by time-resolved resonance fluorescence. Emitted radiation was focused through a calcium fluoride lens and captured by a solar-blind photomultiplier tube orthogonal to both the resonance lamp and the excimer laser. The signals were processed through a multichannel scaler with photon counting and signal averaging. Microwave-powered (90 W) discharge lamps generated resonance radiation; for Cl ($\lambda = 134-140$ nm),[14] a dilution of 0.3% of CCl_4 in Ar flowed continuously through the lamp, while a 0.5% CH_3I/Ar mixture was used for I ($\lambda = 178-206$ nm).[14]

Ar (99.998%, Big Three) bath gas and diluent was taken directly from the cylinder. HI and Cl_2 were synthesized in our laboratory. HI was made by the action of concentrated phosphoric acid on potassium iodide at 343−363 K.[15] The resulting HI was trapped with a methanol slush at about 175 K, and purified several times by low-temperature distillation from 240 K to remove any I_2 impurities, until the final condensed HI was white. The HI was stored in a blackened bulb to prevent photodecomposition. Cl_2 was produced by mixing concentrated HCl and solid KMnO$_4$ at room temperature,[16] and was purified in the same way as HI. The purity of the resulting Cl_2 was checked through its UV−visible spectrum.

HI and Cl_2 were premixed with the flow of Ar before entering the reactor, under "slow flow" conditions. Since the concentration of HI is much higher than the concentration of Cl, the reaction of Cl with HI is pseudo-first order. The analysis of the

---

* marshall@unt.edu.
† Present address: Texas Instruments, Inc., 13553 Floyd Road, Dallas, TX 75265.
‡ Present address: Air Liquide Electronics Chemicals and Services, Inc., 13456 North Central Expressway, Dallas, TX 75243.
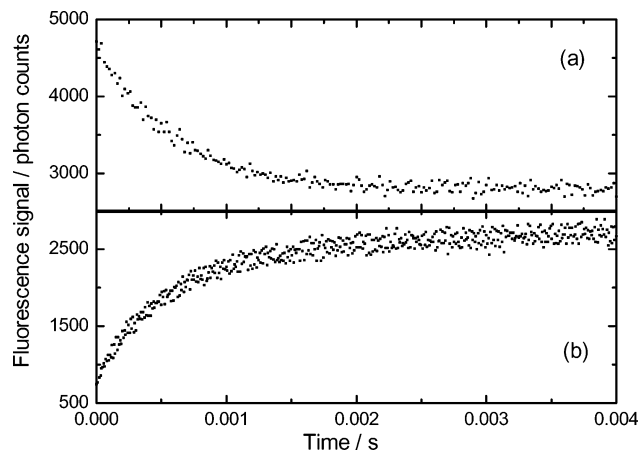
Figure 1. Time profiles of (a) Cl-atom and (b) I-atom fluorescence following 308 nm laser photolysis of Cl_2/HI mixtures at 354 K.
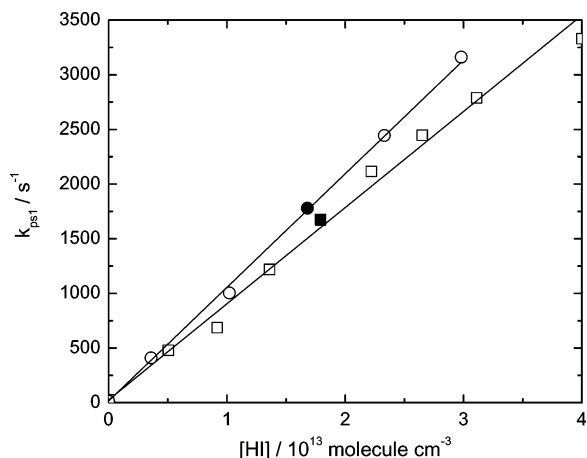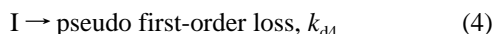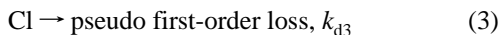

Figure 2. Pseudo-first-order loss rate of Cl measured directly (circles) and from the formation rate of I (squares) in the reaction Cl + HI → HCl + I. The filled symbols correspond to the data of Figure 1.

signals (Cl or I) was carried out with different algorithms, both of them based on the following kinetic scheme, of reaction 1 plus two loss processes:

$$Cl \rightarrow \text{pseudo first-order loss, } k_{d3} \quad (3)$$

$$I \rightarrow \text{pseudo first-order loss, } k_{d4} \quad (4)$$

The decay of Cl is analyzed with a simple exponential function because its concentration is expected to vary as

$$[Cl] = [Cl]_0 \exp(-k_{ps1} t) \quad (5)$$

where $[Cl]_o$ is the initial [Cl]. The pseudo-first-order decay coefficient k_{ps1} is equal to $k_1[HI] + k_{d3}$. The coefficient k_{d3} accounts for the slow loss of Cl other than by reaction 1, which is mainly through diffusion to the reactor walls, and was typically around $15-35$ s^{-1}. The second-order rate constant k_1 is derived as the slope of plots of k_{ps1} vs [HI]. Figure 1a shows a typical Cl decay, and Figure 2 is an example plot of k_{ps1} vs [HI].

Solution of the rate eqs 1, 3, and 4 leads to a double exponential function for the growth and decay of [I]:

$$[I] = B \exp(-k_{d4} t) - C \exp(-k_{ps1} t) \quad (6)$$

where $B = ([I]_0 (k_{ps1} - k_{d4}) + k_1[HI][Cl]_0)/(k_{ps1} - k_{d4})$ and $C = k_1[HI][Cl]_0 /(k_{ps1} - k_{d4})$. After subtraction of the constant
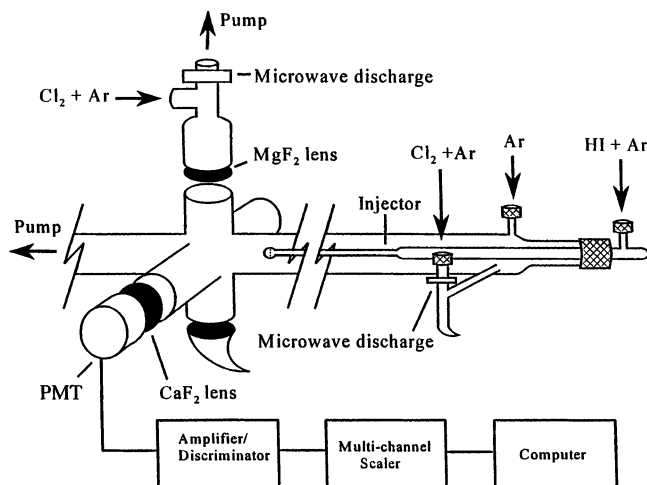

Figure 3. Schematic diagram of the discharge/fast-flow apparatus.

background from scattered light (measured before triggering the photolysis pulse), the four parameters in eq 6 were derived from nonlinear fitting of the I fluorescence signals. Figure 1b shows an example of the growth of I. The coefficient k_1 was obtained as the slope of a plot of k_{ps1} vs [HI], as in the Cl-monitoring experiments. When [HI] = 0, no I is produced, and for this datum k_{ps1} was obtained instead from the loss of Cl. An example is shown in Figure 2. At the highest temperatures, [I] was observed to *increase* slowly following its rapid generation from reaction 1, which corresponds to a negative value for k_{d4}, typically -10 s^{-1}. The origin of this slow growth term for [I] is unclear, but it is numerically well-separated from typical k_{ps1} values of $500-3000$ s^{-1}.

A potential difficulty with these experiments is the loss of HI by adsorption on the reactor walls. This effect was investigated by using two reactors, made of Pyrex and steel, and varying the passivation conditions. Several parameters were varied to check their influence on the rate constants. The average gas residence time before photolysis, τ, was varied by a factor of 2 and the concentration of Cl_2 was changed by a factor of 4. The photolysis energy E and $[Cl_2]$ were varied to give different $[Cl]_0$. The chlorine concentration $[Cl]_0$ was placed on an absolute basis through the absorbed photon flux (calculated from E), the laser beam cross section, and the absorption cross-section of Cl_2 (1.85×10^{-19} cm^2,[17]) combined with a quantum yield of 2 for atomic chlorine.[14]

2.2 Discharge Flow Experiments. A schematic diagram of the flow tube apparatus is shown in Figure 3. The apparatus consists of a 70-cm-long Pyrex flow tube (radius $r = 1.05$ cm). Cl atoms are produced in the sidearm of the flow tube by a microwave discharge (Opthos Instruments, 2450 MHz) through a dilution of Cl_2 in Ar. The second reagent is introduced into the flow tube by means of a moveable injector (o.d. 1.5 cm). The inside of the flow tube is coated with halocarbon wax (Series 1500-Wax, Halocarbon Products Corp.) and the outside of the injector is coated with phosphoric acid to minimize heterogeneous loss of atoms at the surface.[18] About half of the flow of Ar is diverted through the sidearm to push the Cl atoms through the flow tube. Low pressures, around 3.5 mbar, are maintained in the flow tube by a rotary pump (Sargent Welch 1397, 500 L min^{-1}).

The detection region consists of a six-arm cell made of Pyrex glass. One arm of this cell is connected to the flow tube and the opposite arm is connected to the pump. Atomic Cl concentrations are monitored by resonance fluorescence. Vacuum UV fluorescence at $\lambda = 135$ nm is excited by a microwave-

Kinetic Studies of the Cl + HI Reaction

J. Phys. Chem. A, Vol. 108, No. 33, 2004 **6859**

powered discharge lamp connected to one of the arms at right angles to the flow tube, through which a 1% mixture of Cl_2 in Ar is passed. Fluorescence is detected with a solar blind photomultiplier tube (Thorn EMI, model 9423) optically coupled to the six-arm cell via a calcium fluoride lens (f.l. 5.0 cm). Output from the photomultiplier tube is fed to an amplifier-discriminator (MIT, model F-100T), which sends TTL pulses to the computer-controlled multichannel scaler (EG&G Ortec, model ACE-MCS) for photon counting. A Woods horn opposite the discharge lamp minimizes scattered light. The pressure in the flow tube is measured with a capacitance manometer (MKS Instruments, model 122A or 222C) opposite the arm to which the PMT is connected.

Reaction 1 was investigated by monitoring the decay of Cl atoms in the presence of excess molecular reagent on a time scale of 2 to 20 ms. The measurements of k_1 were carried out under approximately pseudo-first-order conditions with [Cl] < [HI] so that [HI] was effectively constant. Cl atoms are lost via reaction 1 and heterogeneous loss on the exposed surface of the injector, characterized by k_{inj}. There is also a constant contribution from the loss of Cl at the surface of the flow tube. Thus, an exponential decay of [Cl] is expected

$$[Cl] = [Cl]_o \exp(-k_{ps1} t - c) \qquad (7)$$

where the residence time t of the mixed gases is l/v; v is the mean gas velocity and l is the distance from the moveable reagent injector tip to the observation window. The loss of Cl at the reactor walls is accounted for by c, which is constant during each set of measurements carried out at fixed v and variable l.

The pseudo-first-order decay constant k_{ps1} is related to the rate constant k_1 via

$$k_{ps1} = k_1[HI] + k_{inj} \qquad (8)$$

Graphs of $\ln [Cl]/[Cl]_o$ vs l are linear with a slope equal to the observed decay coefficient, $k_{ps1,obs}$, at a given [HI].
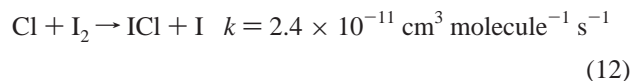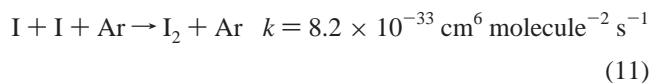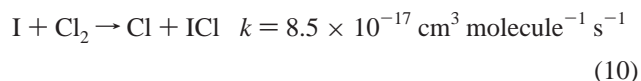
In each experiment, l was varied by 35 cm. The effective first-order rate constant for loss of Cl atoms at the exterior surface of the injector, k_{inj}, was measured at the beginning of each experiment by introducing Cl atoms in the flow tube in the absence of molecular reagent and monitoring the change in [Cl] as the injector was gradually withdrawn. Growth of atomic Cl is expected because of the decreased surface area of the injector exposed to Cl atoms as the injector is moved out of the flow tube. Thus, as the reaction time increases, [Cl] increases, and k_{inj} in eq 8 is negative. The measurement of k_{inj} before each run was followed by passivation of the flow tube using a flow of diluted (~1%) HI over a period of 45 min. The passivation procedure helps to reduce the scatter between kinetic runs. The coefficient k_{inj} is small compared to $k_{ps1,obs}$ and, because it is constant, is separable from $k_{ps1,obs}$. Observation of an increase in k_{inj} is a sign that the injector and wall coatings need to be replaced.

Our experiments were carried out with Reynolds numbers, Re, typically around 100. The length required to develop laminar flow is 0.12 r Re,[19] that is, about 12 cm, so that experiments were performed in regions where laminar flow was close to completely developed. The $k_{ps1,obs}$ values are corrected for effects of diffusion using the relation[20]

$$k_{ps1} = k_{ps1,obs}(1 + k_{ps1,obs} D/v^2 + k_{ps1,obs} r^2/48D) \qquad (9)$$

where D is the diffusion coefficient of atomic Cl in Ar. The first correction term in eq 9 may be identified with axial diffusion,[20] which arises when Cl atoms diffuse down the concentration gradient along the flow tube. The second correction term accounts for radial diffusion of Cl across the flow tube.[20] The value of D is calculated[21] from the Lennard-Jones parameters σ and ϵ/k for Cl (3.36 Å, 328 K) and Ar (3.418 Å, 124 K).[22] Straight-line plots of the corrected k_{ps1} values vs [HI] would have a slope equal to an effective value of the rate constant for reaction 1, and have k_{inj} as the intercept. However, further corrections were made to the k_{ps1} values before obtaining k_1, as outlined below.

A separate set of titration experiments was carried out to determine the absolute Cl atom concentration. The titrations employed reaction 1, with the injector tip kept at the middle of the range of l used in the kinetic runs. Under the titration conditions of long residence time and high [HI], reaction 1 is essentially complete before fluorescence is measured, and the intensity falls to zero when $[HI]_{end point} = [Cl]_o$. These absolute concentrations were employed in simulations of [Cl] vs time profiles taking into account reaction 1, surface loss, and the potentially interfering secondary chemistry

$$I + Cl_2 \rightarrow Cl + ICl \quad k = 8.5 \times 10^{-17} \text{ cm}^3 \text{ molecule}^{-1} \text{ s}^{-1} \qquad (10)$$

$$I + I + Ar \rightarrow I_2 + Ar \quad k = 8.2 \times 10^{-33} \text{ cm}^6 \text{ molecule}^{-2} \text{ s}^{-1} \qquad (11)$$

$$Cl + I_2 \rightarrow ICl + I \quad k = 2.4 \times 10^{-11} \text{ cm}^3 \text{ molecule}^{-1} \text{ s}^{-1} \qquad (12)$$

with literature values for the 298-K rate constants.[6,23,24] The conditions (concentrations of species, residence time) were the same as those used for the kinetic runs, and simulation of each ([Cl], l) point is carried out with the ACUCHEM program[25] to yield a time profile of atomic chlorine. The slope of a $\ln([Cl]/[Cl]_0)$ vs t plot provides a model k_{ps1} value for the particular measurement, which was then divided by the initial concentration of HI to yield an effective second-order rate constant, k_{model}. The correction factor for each experimental measurement can then be written as k_{input}/k_{model}, where k_{input} is the value of the rate constant put into the simulation. We used $k_{input} = 9.5 \times 10^{-11} \text{ cm}^3 \text{ molecule}^{-1} \text{ s}^{-1}$. Each experimental k_{ps1} value (already corrected for diffusion via eq 9) was multiplied by the appropriate correction factor, and then plotted against [HI] to yield the final corrected rate constant k_1. Figure 4 is an example.

3. Results and Discussion

Table 1 summarizes the laser photolysis measurements for CI + HI under different experimental conditions between temperatures of 296 and 390 K. The listed standard deviations reflect the 1σ statistical uncertainties in the slopes of plots such as Figure 2, combined in quadrature with a 5% 1σ allowance for instrumental errors. It took at least 20 min for a flow of HI to saturate the surface of the steel reactor. Alternatively, a few mbar of pure HI was incubated in the reactor for an hour before starting the measurements. Under these two conditions, the measured rate constants were close to the values obtained with the Pyrex reactor. There was no significant change in the rate constant with the photolysis energy or [Cl]₀, which indicates that secondary reactions with products or other photolysis fragments are negligible. As may be seen in Figure 2 and in

TABLE 1: Summary of Laser Photolysis Measurements on HI + Cl

T, K	P, mbar	τ_{res}, s	[HI], 10^{13} molecule cm^{-3}	[Cl$_2$], 10^{13} molecule cm^{-3}	laser E, mJ	[Cl]$_0$, 10^{12} molecule cm^{-3}	monitored atom	$k_1 \pm \sigma_{k1}$, 10^{-10} molecule^{-1} cm^3 s^{-1}
296	45.9	0.4	0.7–3.3	22.0	43	1.8	Cl	1.07 ± 0.07
296	31.1	0.5	0.5–1.8	15.6	43	1.3	Cl	1.01 ± 0.05
297	38.7	0.6	0.8–2.8	5.1	58	0.6	Cl	0.93 ± 0.06^b
297	38.7	0.7	0.6–2.2	12.1	58	1.3	Cl	0.96 ± 0.05^b
297	39.1	0.8	1.9–6.9	11.8	47	1.0	I	1.04 ± 0.09^b
297	38.1	0.8	0.9–5.4	14.8	43	1.2	I	1.05 ± 0.07^b
297	38.1	0.8	0.9–5.4	14.8	43	1.2	I	1.05 ± 0.09^b
297	44.4	0.7	1.1–5.3	12.2	40	0.9	I	1.03 ± 0.07^b
297	44.5	0.7	1.1–5.3	24.0	40	1.8	I	1.14 ± 0.12^b
297								1.01 ± 0.02^a
319	39.9	0.8	1.0–5.7	16.6	50	1.6	I	1.13 ± 0.06
319	39.7	0.4	0.8–4.3	8.1	50	0.8	I	0.82 ± 0.05
319	39.9	0.4	0.8–3.6	16.1	50	1.6	I	1.22 ± 0.10
319								0.98 ± 0.04^a
344	40.0	0.8	0.7–3.3	14.2	43	1.1	I	1.22 ± 0.13
344	40.9	0.4	0.5–3.1	7.2	43	0.6	I	1.07 ± 0.07
344								1.10 ± 0.06^a
353	41.3	0.4	0.7–3.3	19.6	36	1.3	Cl	1.10 ± 0.06
353	41.3	0.4	0.4–3.0	19.6	36	1.3	Cl	1.04 ± 0.06
354	31.6	0.4	0.5–4.0	8.8	58	1.0	I	0.88 ± 0.05
354	46.3	0.3	0.7–4.0	6.6	58	0.7	I	0.79 ± 0.05
354								0.93 ± 0.03^a
381	38.0	0.3	0.6–3.0	13.3	40	1.0	I	0.60 ± 0.04
381	37.7	0.3	0.7–3.4	13.2	40	1.0	I	0.71 ± 0.05
386	41.3	0.4	0.7–4.2	7.0	54	0.7	I	0.70 ± 0.05
386	41.3	0.4	1.1–5.1	14.9	54	1.5	I	0.77 ± 0.06
390	41.2	0.3	0.9–4.8	14.6	40	1.1	I	0.86 ± 0.05
390	41.3	0.7	0.9–4.0	14.6	40	1.1	I	0.90 ± 0.08
390	41.3	0.7	0.9–4.0	28.7	40	2.1	I	0.99 ± 0.07
386								0.75 ± 0.02^a

^{a} Weighted average for each temperature (see text). ^{b} Measurements were made in the Pyrex reactor.

Figure 4. Plot of pseudo first-order loss rate of Cl in the presence of excess HI in the fast-flow reactor.

Figure 5. Arrhenius plot of rate constants for the Cl + HI reaction. Solid circles and line, laser photolysis, present work (error bars are 2σ); open downward pointing triangle, flow tube, present work; open square, Wodarczyk and Moore;[3] open upward pointing triangle, Mei and Moore;[4] asterisks, Mei and Moore;[5] open circle, Dolson and Leone;[6] solid triangle, Iyers et al.[7]

Table 1, similar rate constants are obtained via monitoring of either Cl or I. The agreement is excellent at room temperature, while the deviations are up to around 20% at 354 K. Given the overall scatter in the data and potential systematic errors, discussed below, this is good agreement. Therefore, all data were combined at each temperature.

The Arrhenius plot of the Cl + HI reaction obtained in this study and previous measurements by other techniques are shown in Figure 5. Each point in the graph from this study is the weighted mean for that temperature. As outlined by Bevington,[26] we weight each value as $w_i = 1/\sigma_i^2$, and obtain the mean μ and its standard deviation σ_μ via the relations $\mu = \Sigma w_i x_i/\Sigma w_i$ and $\sigma_\mu^2 = 1/\Sigma w_i$. The error bars in Figure 5 are 2σ, and it may be seen that this purely statistical quantity accounts for much of the scatter in the Arrhenius plot. The best fit of the laser-
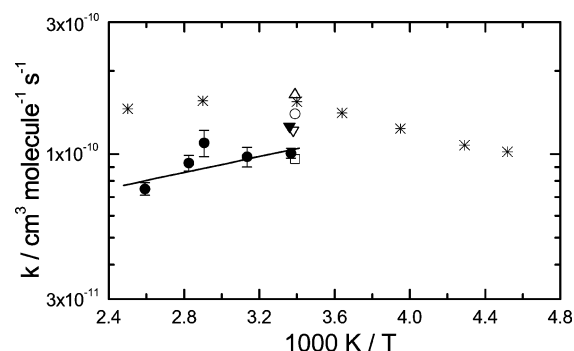
photolysis/resonance fluorescence data is

$$k_1 = (3.4 \pm 1.4) \times 10^{-11} \exp(+2.8 \pm$$
$$1.1 \text{ kJ mol}^{-1}/RT) \text{ cm}^3 \text{ molecule}^{-1} \text{ s}^{-1} \quad (13)$$

where the errors are 1σ. Since the negative activation energy is not far from zero, an alternative summary of the data over 296–390 K is the weighted mean of the measurements, $k_1 = 0.90 \times 10^{-10}$ cm^3 molecule^{-1} s^{-1}. Consideration of the covariance and the 1σ errors in eq 13 gives an estimated 1σ statistical uncertainty of up to 8% in k_1. With allowance for possible systematic errors in temperature, pressure, and flow, we suggest 95% confidence limits of $\pm$ 19% for k_1.

Table 2 summarizes the discharge-flow measurements. The column headed $k_{1,obs}$ indicates what would be obtained from a

Kinetic Studies of the Cl + HI Reaction

J. Phys. Chem. A, Vol. 108, No. 33, 2004 **6861**

TABLE 2: Summary of Discharge-flow Kinetic Data for HI + Cl

T, K	P, mbar	v, cm s^{-1}	[HI], 10^{12} molecule cm^{-3}	initial [Cl$_2$], 10^{12} molecule cm^{-3}	[Cl], 10^{12} molecule cm^{-3}	k_{inj}, s^{-1}	$k_{1,obs} \pm \sigma_{k1,obs}$,[a] 10^{-11} cm^3 molecule^{-1} s^{-1}	$k_1 \pm \sigma_{k1}$, 10^{-11} cm^3 molecule^{-1} s^{-1}
298	3.5	1946	1.9–5.3	0.9	0.6	−46	8.9 ± 0.5	11.8 ± 1.4
298	3.5	1960	1.5–4.4	1.1	0.8	−23	9.4 ± 0.2	13.2 ± 3.4
297	3.5	1915	2.5–7.2	1.0	0.7	−28	9.1 ± 0.2	12.9 ± 3.0
297	3.6	1860	1.2–5.4	1.5	1.0	−36	9.0 ± 0.3	13.2 ± 1.3
297	3.6	1843	1.4–4.3	1.4	0.9	−35	8.4 ± 1.0	10.5 ± 1.8
297	3.6	1843	3.3–6.7	2.3	1.5	−35	8.7 ± 1.2	13.8 ± 2.7
297	3.6	1850	1.8–6.7	1.1	0.7	−13	7.0 ± 0.7	11.0 ± 1.3
297	3.6	1850	2.7–8.0	2.1	1.4	−13	8.4 ± 0.6	13.3 ± 1.8

[a] $k_{1,obs}$ is the apparent value of k_1 that would be obtained if $k_{ps1,obs}$ (uncorrected for diffusion or stoichiometry) was plotted vs [HI].

plot of uncorrected $k_{ps1,obs}$ values vs [HI]. The ±1σ values quoted are the statistical uncertainties in the slope of this kind of plot. The calculated Cl-atom diffusion coefficient is $D = 0.157(1 \text{ bar}/P)$ cm^2 s^{-1}. The axial term of eq 9 yields minor corrections from 0.3 to 6% to individual k_{ps1} values. The radial term has a larger impact, up to 35% on the largest k_{ps1} values. The measured absolute [Cl] shows that around a third of the Cl$_2$ introduced through the microwave discharge was dissociated. The kinetic simulation indicates that secondary chemistry had a negligible impact, but that stoichiometric correction to individual k_{ps1} values obtained at the lowest [HI]:[Cl] ratios could be as large as 60% (although usually much smaller). Because these corrections are largest for the lowest k_{ps1} values, the impact on k_1 was moderate, up to 16%. The dominant correction term is the radial component of eq 9. The final column of Table 2 lists k_1 values derived by incorporating all these corrections, and the ±1σ values quoted are the statistical uncertainties combined in quadrature with a 10% (1σ) allowance for uncertainty in the corrections. The weighted mean rate constant at 298 K is $k_1 = (1.22 \pm 0.06) \times 10^{-10}$ cm^3 molecule^{-1} s^{-1}, where the quoted error is ±1σ in the mean. Allowance for potential systematic errors yields 95% confidence limits of ± 0.2×10^{-10} cm^3 molecule^{-1} s^{-1}. This flow tube determination of k_1 agrees with our photolysis measurements.

At room temperature, hard-sphere collision theory combined with standard diameters for Cl and HI of 3.4 and 4.1 Å,[27] respectively, yields a collision rate of 2.1×10^{-10} cm^3 molecule^{-1} s^{-1}. Comparison with the measured k_1 implies that reaction occurs very readily, at about 1 out of 2 collisions, and therefore there is little or no energy barrier, consistent with the observed lack of temperature dependence.

In 1974 Wodarczyk and Moore[3] determined the absolute rate constant of this reaction at 295 K by photolyzing Cl$_2$ with laser pulses and monitoring the reaction via the time-resolved IRCL of the vibrationally excited product, HCl. The average value of the rate constant obtained for Cl + HI was $(9.6 \pm 2.4) \times 10^{-11}$ cm^3 molecule^{-1} s^{-1}, in good agreement with this study. Three years later, a new rate constant, 1.64×10^{-10} cm^3 molecule^{-1} s^{-1}, for the Cl + HI reaction was reported by the same group[4] with supposedly more accurate [HI] determination and less wall-catalyzed interference, although this value seems somewhat high. The only published temperature dependence of k_1 was obtained by Mei and Moore,[5] and was also based on IRCL measurements. The observed reaction rates showed almost no temperature dependence around a temperature range comparable to the present study, although a significant variation of k_1 was seen at lower temperatures. Dolson and Leone[6] studied the kinetics of the slow chain of reactions 1 and 10 by real-time detection of IRCL from vibrationally excited HCl. Cascading fluorescence was observed from individual vibrational levels. A rate constant of $(1.4 \pm 0.3) \times 10^{-10}$ cm^3 molecule^{-1} s^{-1} was obtained, which agrees with the present study. A different approach is illustrated

by the study of Iyer et al.[7] They measured the rate constant for removal of Cl by HI relative to C$_2$H$_6$ using a competitive radiochemical technique, and derived $k_1 = (1.26 \pm 0.14) \times 10^{-10}$ cm^3 molecule^{-1} s^{-1}.

With respect to the issues raised by Dobis and Benson[11] noted in the Introduction, small values for Cl diffusive loss, typically up to a few percent of the overall consumption (see Figure 2), mean that any uncertainty here has a negligible impact, and that in this system there was no major loss pathway for Cl that did not lead to I formation. The accord to within roughly 20% between the three approaches applied here, approaches that vary as to monitored species and bath gas pressure regime, is consistent with experimental uncertainties. The general accord with other prior determinations further suggests that all methods are consistent for reaction 1. This implies that any excess translational or electronic excitation in the photolytically produced Cl atoms does not appreciably change the kinetics relative to Cl atoms generated in the discharge/fast-flow system. Further, in the flow system the reacting mixture is not exposed to actinic radiation from a resonance lamp until the detection region, unlike the pulsed photolysis system.

Conclusions

Three different methods to determine the rate constant k_1 for Cl + HI → HCl + I are consistent, and agree with most previous literature data. This indicates that, at least for this system, the approach of monitoring the growth of the atomic halogen product in reactions of the type R + HX → RH + X appears to be reliable.

References and Notes

(1) Maylotte, D. H.; Polanyi, J. C.; Woodall, K. B. *J. Chem. Phys.* **1972**, *57*, 1547.
(2) Levine, R. D.; Bernstein, R. B. *Molecular Reaction Dynamics and Chemical Reactivity*; Oxford University Press: New York, 1987, Ch. 1.
(3) Wodarczyk, F. J.; Moore, C. B. *Chem. Phys. Lett.* **1974**, *26*, 484.
(4) Mei, C. C.; Moore, C. B. *J. Chem. Phys.* **1977**, *67*, 3936.
(5) Mei, C. C.; Moore, C. B. *J. Chem. Phys.* **1979**, *70*, 1759.
(6) Dolson, D. A.; Leone, S. R. *J. Chem. Phys.* **1982**, *77*, 4009.
(7) Iyer, R. S.; Rogers, P. J.; Rowland, F. S. *J. Phys. Chem.* **1983**, *87*, 3799.
(8) Seakins, P. W.; Pilling, M. J. *J. Phys. Chem.* **1991**, *95*, 9874.
(9) Nicovich, J. M.; Van Dijk, C. A.; Kreutter, K. D.; Wine, P. H. *J. Phys. Chem.* **1991**, *95*, 9890.
(10) Kalinovski, I. J.; Gutman, D.; Krasnoperov, L. N.; Goumri, A.; Yuan, W.-J.; Marshall, P. *J. Phys. Chem.* **1994**, *98*, 9551.
(11) Dobis, O.; Benson, S. W. *J. Am. Chem. Soc.* **1995**, *117*, 8171.
(12) Shi, Y.; Marshall, P. *J. Phys. Chem.* **1991**, *95*, 1654.
(13) Ding, L.; Marshall, P. *J. Phys. Chem.* **1992**, *96*, 2197.
(14) Okabe, H. *Photochemistry of Small Molecules*; Wiley: New York, 1978.

6862 *J. Phys. Chem. A, Vol. 108, No. 33, 2004*

Yuan et al.

(15) Vogel, A. I. *Textbook of Macro and Semimicro Qualitative Inorganic Analysis*, 4th ed.; Longmans, Green, and Co.: London, 1954.

(16) *Mellor's Modern Inorganic Chemistry*; Parkes, G. D., Ed.; Wiley: New York, 1967.

(17) DeMore, W. B.; Sander, S. P.; Golden, D. M.; Hampson, R. F.; Kurylo, M. J.; Howard, C. J.; Ravishankara, A. R.; Kolb, C. E.; Molina, M. J. *Chemical Kinetics and Photochemical data for Use in Stratospheric Modeling. Evaluation Number 12*; JPL: Pasadena, 1997.

(18) Clyne, M. A. A.; MacRafert, A. J.; Murrells, T. P.; Stief, L. J. *J. Chem. Soc., Faraday Trans. 2* **1984**, *80*, 877.

(19) Padet, J. *Fluides en Encoulement. Methodes et Modeles.*; Masson: Paris, 1991.

(20) Keyser, L. F. *J. Phys. Chem.* **1984**, *88*, 4750.

(21) Reid, R. C.; Sherwood, T. K. *The Properties of Gases and Liquids*; McGraw-Hill: New York, 1958.

(22) Vandooren, V.; Fristrom, R. M.; Tiggelen, P. J. V. *Bull. Soc. Chim. Belg.* **1992**, *101*, 901.

(23) Baulch, D. L.; Duxbury, J.; Grant, S. J.; Montague, D. C. *J. Phys. Chem. Ref. Data* **1981**, *10*.

(24) Kuznetsova, S. V.; Maslov, A. I. *Khim. Fiz.* **1987**, *6*, 1554.

(25) Braun, W.; Herron, J. T.; Kahaner, D. *Int. J. Chem. Kinet.* **1988**, *22*, 51.

(26) Bevington, P. R. *Data Reduction and Error Analysis for the Physical Sciences*; McGraw-Hill: New York, 1969, Ch. 5.

(27) Hirschfelder, J. O.; Curtis, C. F.; Bird, R. B. *Molecular Theory of Gases and Liquids*; Wiley: New York, 1954.